

540 Supporting Information

541 **Neutrophils Enable Local and Non-Invasive Liposome Delivery to Inflamed Skeletal** 542 **Muscle and Ischemic Heart**

543 *Junyi Che, Adrian Najer, Anna K. Blakney, Paul F. McKay, Mohamed Bellahcene, Charles*
544 *W. Winter, Amalia Sintou, Jiaqing Tang, Timothy J. Keane, Michael D. Schneider, Robin J.*
545 *Shattock, Susanne Sattler, Molly M. Stevens**

546 J. Che, Dr. A. Najer, Dr. C. W. Winter, J. Tang, Dr. T. J. Keane, Prof. M. M. Stevens
547 Department of Materials, Department of Bioengineering, and Institute of Biomedical
548 Engineering, Imperial College London, London, SW7 2AZ, United Kingdom

549
550 Dr. A. K. Blakney, Dr. P. F. McKay, Prof. R. J. Shattock
551 Department of Infectious Diseases, Imperial College London, London, W2 1PG, United
552 Kingdom

553
554 A. Sintou, Dr. S. Sattler
555 National Heart and Lung Institute, Imperial College London, London, W12 0NN, United
556 Kingdom

557
558 Dr. M. Bellahcene, Prof. M. D. Schneider
559 British Heart Foundation Centre of Research Excellence, National Heart and Lung Institute,
560 Imperial College London, London W12 0NN, United Kingdom

561
562 *Corresponding author email address:

563 m.stevens@imperial.ac.uk

564

565 **Supplementary Experimental Section**

566 *Isolation and characterisation of murine neutrophils from mouse bone marrow*

567 Mouse neutrophils were isolated from bone marrow by negative selection using a neutrophil
568 isolation kit (Miltenyi Bio). Briefly, bones from mouse legs were immersed in RPMI 1640
569 medium after muscle removal. Mouse bone marrow cells were flushed out with buffer solution
570 (0.5% (w/v) bovine albumin and 2 mM EDTA), filtered through the cell strainer, centrifuged at
571 400 g for 10 min and resuspended in the buffer solution. A cocktail of biotin-conjugated
572 monoclonal antibodies was added to bind to non-target cells, followed by multiple washing
573 steps. The secondary labelling reagent, anti-biotin monoclonal antibodies conjugated to
574 Microbeads, was added and magnetically labelled non-target cells were depleted by retaining

575 them within a MACS Column in the magnetic field of a MACS Separator, allowing unlabelled
576 neutrophils to run through the column. The yield was determined by using a haemocytometer
577 and the cell viability was calculated by trypan blue exclusion. The purity of isolated neutrophils
578 was measured using immunofluorescence antibodies staining with PE anti-mouse CD11b (250
579 ng mL⁻¹, BioLegend) and APC anti-mouse Ly6G/Ly6C (250 ng mL⁻¹, BioLegend). Then, the
580 morphology of neutrophils was visualised under the widefield microscope (Zeiss Axio
581 Observer) using Giemsa-Wright stain.

582 *Preparation and characterisation of MTX-liposome/neutrophils*

583 MTX loaded liposomes composed of 16:0-18:1 PC (POPC), 18:0 TAP (Avanti Polar Lipid) and
584 cholesterol (Sigma) (44:16:40, w:w:w) were prepared using a thin-film hydration method.^[1]
585 MTX (Sigma) solutions at 5 mg mL⁻¹ and 10 mg mL⁻¹ in PBS were added to hydrate the film,
586 followed by extrusion through membrane filters with a pore size of 100 nm. Free MTX was
587 removed using two sequential size exclusion chromatography (PD-10 desalting columns, GE
588 Healthcare) and purified MTX-loaded liposomes were used for all the subsequent studies.
589 Dynamic light scattering (DLS) was used to measure the hydrodynamic diameter and zeta
590 potential of liposomes (Malvern, Zetasizer). The size of MTX-liposomes was further confirmed
591 by transmission electron microscopy (TEM). MTX-liposomes were dropped onto a cooper grid
592 (CF400-Cu, Electron Microscopy Science) and stained with 2% fresh ammonium molybdate.
593 After air-dry, the sample was imaged by TEM (JEOL 2100F).^[2] The release of MTX from
594 liposomes was measured using a dialysis tube (Spectra-Por, 5 mL, MWCO 100 kDa) in PBS
595 pH 7.4 at room temperature. To mimic the release of MTX from liposomes in the extracellular
596 environment at the inflammatory site, MTX-liposomes were incubated in 90% FBS (v/v) for 8
597 h and then transferred to a dialysis tube (Spectra-Por, 1 mL, MWCO 300 kDa). After an
598 additional 12 h and 44 h dialysis in PBS, the amount of retained MTX inside liposomes in the
599 dialysis tube was quantified using Methotrexate ELISA kit (Enzo). The liposome solution

600 inside the tube was collected at different time points and the retained amount of MTX in
601 liposomes was measured by LC-MS. The LC-MS system consisted of an Agilent Technologies
602 1260 Infinity, coupled to an Agilent 6130 Series Quadrupole spectrometer (electrospray
603 ionization mode, ESI+). All the analysis were carried out using a Gemini NX column (5 micron
604 pore size, 150 x 4 mm). A flow rate of 1 mL min⁻¹ and a gradient of (10-90)% B over 10 min
605 were used. Eluent A: water/0.1% NH₃.H₂O; eluent B: acetonitrile/0.1% NH₃.H₂O. UV detection
606 was performed at 272 nm in a scan mode ranging from 100 to 1000 m/z. MTX eluted at t = 2.01
607 min (m/z = 455[M+H]⁺). The corresponding UV peak at λ=272 nm was integrated and used for
608 quantification based on established standard curve.

609 MTX-liposome/neutrophils were prepared by incubating neutrophils with MTX-liposomes.
610 Briefly, isolated neutrophils were placed in a DNA low bind tube, followed by incubating with
611 MTX-liposomes (MTX concentration used to hydrate lipid film: 5 mg mL⁻¹ and 10 mg mL⁻¹;
612 final lipid concentration: 1 mg mL⁻¹ and 2 mg mL⁻¹) for 1h. After centrifugation and washing
613 with PBS three times, MTX-liposome/neutrophils were resuspended in PBS and ready for
614 subsequent experiments. Neutrophils uptake efficiency of MTX-liposomes was measured by
615 using flow cytometry (BD FACSCanto, BD Biosciences) and the location of MTX-liposomes
616 (liposomes were labelled with DiD) was observed using confocal laser scanning microscopy
617 (CLSM, Leica SP5/MP) and Zeiss PS1 Elyra microscope. Multi-channel 3D SIM images were
618 reconstructed from five rotational widefield acquisitions at each imaging plane using Zen
619 software. Neutrophil viability after 4 h and 8 h incubation with MTX-liposomes was measured
620 using Zombie Green Fixable Viability Kit (Biolegend) by flow cytometry. In order to quantify
621 the loading amount of MTX, MTX-liposome/neutrophils were sonicated in buffer solution and
622 the MTX amount was quantified by using Methotrexate ELISA kit (Enzo).

623 *Evaluation of physiological functions of neutrophils after loading with MTX-liposomes*

624 Three different physiological functions of neutrophils were evaluated before and after loading
625 with liposomes, including CD11b protein expression on the neutrophil cell surface, superoxide-
626 anion generation, and cell migration. Blank neutrophils and MTX-liposome/neutrophils were
627 treated with different concentrations of fMLP at 37 °C for 30 min. After centrifugation and
628 washing with PBS three times, PE anti-mouse CD11b (250 ng mL⁻¹, BioLegend) was added to
629 conjugate to protein for 30 min and then washed with PBS three times. 4% of PFA was added
630 to fix cells. The fluorescence intensity was measured using flow cytometry (BD FACSCanto,
631 BD Bioscience).

632 Blank neutrophils and MTX-liposome/neutrophils were treated with fMLP (1 μM) at 37 °C for
633 30 min. After washing with PBS three times, the cells were incubated with dihydroethidium
634 (10 μM, MedChemExpress) at 37 °C for 30 min. After centrifugation and washing with PBS
635 three times, the fluorescence intensity was measured using flow cytometry to determine the
636 superoxide-generation ability of neutrophils after loading with MTX-liposomes.

637 The migration ability of MTX-liposome/neutrophils was determined using a transwell cell
638 migration method. Cell culture inserts were put into the cell plate. Blank neutrophils and MTX-
639 liposome/neutrophils were added into cell culture inserts (polycarbonate membrane, 3.0 μm
640 pore size, 6.5 mm membrane diameter, 0.33 cm² surface area) (upper chambers) and meanwhile,
641 wells of the plate (lower chambers) were filled with different concentrations of fMLP (1 nM
642 and 100 nM). After 3 h, cell culture inserts were taken out and cells on the upper side of the
643 membrane were removed. The cells on the bottom side of the membrane were stained with
644 DAPI, imaged and counted under bright field. CLSM was used to observe the MTX-liposomes
645 (liposomes were labelled with DiD) in the migrated neutrophils.

646 *Stimulated release of MTX-liposomes from neutrophils*

647 NETs formation of neutrophils after treating with PMA was imaged using CLSM. Liposomes
648 were labelled with DiD, followed by incubation with neutrophils to form liposome loaded
649 neutrophils. Formulated liposome loaded neutrophils were incubated in the presence of fMLP
650 or PMA for 0 h and 8 h. Released DNA fragments were stained with PI. 4% PFA was used to
651 fix samples and DAPI was used later to stain for cell nuclei. CLSM was used to image the
652 samples.

653 The stimulated release of MTX-liposomes from neutrophils was determined using Fluorescence
654 correlation spectroscopy (FCS). MTX-liposome/neutrophils (liposomes were labelled with DiD)
655 were treated with or without PMA for 8 h, followed by centrifugation to collect the supernatant.
656 FCS measurements were run to detect the amount and properties of liposomes after release from
657 neutrophils. FCS was performed on a commercial LSM 880 (Carl Zeiss, Jena, Germany)
658 equipped with an incubation chamber set to 37°C. A HeNe laser at 633nm was used as
659 excitation source combined with an appropriate filter set to detect the fluctuating fluorescence
660 signal. As objective, we used a 40x C-Apochromat water immersion objective (numeric
661 aperture of 1.2). Glass-bottom ibidi 8-well plates (80827, ibidi, Germany) were used to place 5
662 µl sample droplets and measurements were conducted 200 µm above the glass plate. Alexa647
663 in PBS was used as a standard to calibrate the beam waist ($D = 3.3 \times 10^{-6} \text{ cm}^2/\text{s}$ (Alexa647) at
664 25°C was corrected for the higher temperature used: $D = 4.42 \times 10^{-6} \text{ cm}^2/\text{s}$ at 37°C).^[3] Intensity
665 traces of 30 x 5s were recorded per sample. In the figures, we always plotted the full intensity
666 curve and the average autocorrelation curves across the whole measurement (both 150 s).
667 Autocorrelation was performed on ZEN software (Carl Zeiss, Jena, Germany) and data was
668 exported for fitting and analysis using PyCorrfit program 1.1.6.^[4] using one component fits:

669
$$G_{1comp}(\tau) = \left(1 + \frac{T}{1-T} e^{\frac{-\tau}{\tau_{trip}}}\right) * \frac{1}{N * \left(1 + \frac{\tau}{\tau_D}\right) * \sqrt{1 + \frac{\tau}{SP^2 \tau_D}}}$$

670 N refers to the effective number of diffusing species in the confocal volume with a height to
671 weight ratio (structural parameter SP) fixed to 5. τ_{trip} is the triplet time with corresponding
672 triplet fraction T , and τ_D is the diffusion time.

673 The x-y dimension of the confocal volume (ω_{xy}^2) was calibrated using the calibration solution
674 of Alexa647 in PBS. Diffusion coefficients (D) for the sample measurements were then
675 obtained by plugging in the calculated diffusion times (τ_D) from above:

$$676 \quad D = \frac{\omega_{xy}^2}{4\tau_D}$$

677 Einstein-Stokes equation was subsequently used with the obtained diffusion coefficients (D) to
678 calculate hydrodynamic radii (R_h).

679 The amount of MTX in the released particle solution after incubation of loaded neutrophils in
680 the presence of PMA was quantified using Methotrexate ELISA kit (Enzo). Formulated MTX-
681 liposome/neutrophils were incubated with and without PMA for 8 h. The supernatants were
682 collected at 0 h, 4 h and 8 h time points and the amount of MTX was measured by Methotrexate
683 ELISA kit. The percentage of released MTX was calculated by MTX amount (at different time
684 points)/MTX amount (initial loading).

685 *Co-culture of MTX-liposome/neutrophils with RAW 264.7 cells*

686 To further demonstrate the transport of liposomes from neutrophils to target cells, RAW 264.7
687 cells were used as the target cell line to co-culture with liposome loaded neutrophils. In order
688 to distinguish RAW 264.7 cells from neutrophils, CellTracker Green CMFDA Dye
689 (ThermoFisher) was used to label the cytoplasm of RAW 264.7 cells. Neutrophils were
690 incubated with liposomes for 1 h and free liposomes were washed away by centrifugation.
691 Labelled RAW 264.7 cells were then added to co-culture with formulated liposome loaded

692 neutrophils in FBS free medium containing PMA (100 nM). After 8 h incubation, cell samples
693 were fixed and measured by flow cytometry.

694 To image the release of liposomes from neutrophils in responding to PMA-induced NETs
695 formation and the re-uptake of released liposomes by RAW 264.7 cells, liposome loaded
696 neutrophils and RAW 264.7 cells were cultured together in the presence of PMA and observed
697 by CLSM. RAW 264.7 cells were seeded in the ibidi 8-well plate. After overnight incubation,
698 DiD-liposome/neutrophils (0.3×10^6 neutrophils) were added to RAW 264.7 cells and incubated
699 in the medium with or without PMA (100 nM). At 4 h and 8 h incubation time point, RAW
700 264.7 cells were washed with PBS to remove suspended neutrophils in the medium and stained
701 with propidium iodide (PI, $5 \mu\text{g mL}^{-1}$) for 30 min. DAPI was used to stain for cell nuclei.

702 To investigate the biological effect of MTX-liposome/neutrophils system on target cells, cell
703 proliferation was chosen as the outcome to measure after incubating with MTX-
704 liposome/neutrophils containing different inflammatory cytokines. RAW 264.6 cells were
705 chosen as the targeted cells and were seeded in the 96-well plate (2×10^4 cells/well). After 12 h
706 incubation, MTX-liposome/neutrophils were added into each well with growth medium
707 containing LPS and PMA. In this case, LPS (100 ng mL^{-1}) was used to mimic the inflammatory
708 environment and PMA was used to induce neutrophil forming NETs to release encapsulated
709 MTX-liposomes. After 24 h incubation, neutrophils were washed away with PBS and the
710 viability of RAW 264.7 cells was measured using Cell Counting Kit-8 (Sigma Aldrich).

711 *Animals*

712 All animals were handled in accordance with the UK Home Office Animals Scientific
713 Procedures Act 1986 and with an internal ethics board and UK government approved project
714 (P63FE629C) and personal license (IC37CBB8F) for LPS-injury skeletal muscle model, project
715 (PD359F318) and personal license (I6D2D5295) for myocardial IRI model. Food and water

716 were supplied *ad libitum*. Female BALB/c mice (Charles River, UK) 6-8 weeks (treatment mice)
717 or 10-12 weeks (donor mice) of age were placed into groups (n = 5) and housed in a fully
718 acclimatized room, used for LPS-injury skeletal muscle model. Female CD1 mice (Charles
719 River, UK) 4-5 weeks (treatment mice) or 8-10 weeks (donor mice) of age were placed into
720 groups (n = 5) and housed in a fully acclimatized room, used for myocardial IRI model.

721 *LPS-injury skeletal muscle model and in vivo neutrophil migration and anti-inflammation*
722 *treatment studies*

723 LPS-biotin/streptavidin particles were prepared by complexing biotinylated LPS elementary
724 bodies (LPS Biotin-EB, Invivogen, France) with streptavidin from *Streptomyces avidinii*
725 (Sigma, UK) at a ratio of 1:4 biotin:streptavidin (w/w) in PBS. Mice were injected
726 intramuscularly in the right quadriceps with 50 µg of particles (10 µg LPS Biotin EB, 40 µg
727 streptavidin) in 50 µL, while the left quadriceps was not injected to serve as an internal control.

728 To investigate the migration ability of injected neutrophils to the inflamed quadriceps, 24 h
729 after LPS injection, isolated neutrophils from donor mice (labelled with VivoTrack 680) were
730 intravenously injected to LPS treated mice (4×10^6 per mouse). 1 h, 2 h and 4 h post i.v.
731 injection, mice were sacrificed and quadriceps from both legs were taken out. Quadriceps were
732 digested using 2 mL of Dulbecco's Modified Eagle's Medium supplemented with 1 mg mL^{-1}
733 collagenase P (Sigma, UK) and 5 mg mL^{-1} dispase II (Sigma, UK) for 30 min and smashed
734 through the cell strainer to obtain a single cell suspension. The cell suspension was then stained
735 with Fixable Aqua Dead cell stain (Thermo Fisher, UK) diluted 1:400 for 20 min and neutrophil
736 surface markers PE anti-mouse CD11b (250 ng mL^{-1}) and Alexa 488 anti-mouse Ly6G/Ly6C
737 (250 ng mL^{-1} , Biolegend) for 30 min. Cells were fixed with 3% PFA and measured using flow
738 cytometry.

739 To investigate the migration ability of neutrophils after loading with liposomes, 24 h after LPS
740 injection, formulated liposome/neutrophils (liposomes were labelled with DiI and neutrophils
741 were labelled with VivoTrack 680) were intravenously injected to LPS injected mice. 1 h post
742 i.v. injection, mice were sacrificed and quadriceps from both legs were taken out. A single cell
743 suspension was obtained as described above and then stained with Aqua Dead cell stain and
744 neutrophil surface markers PerCP anti-mouse CD11b (250 ng mL⁻¹) and Alexa 488 anti-mouse
745 Ly6G/Ly6C (250 ng mL⁻¹). Cells were fixed with 1.5% PFA and measured using flow
746 cytometry.

747 To demonstrate the anti-inflammation treatment effect of liposome/neutrophils system, MTX
748 was loaded in liposomes (10 mg mL⁻¹ MTX was used during liposome formation) and MTX-
749 liposome/neutrophils were formulated as described above. 24 h after LPS injection, formulated
750 MTX-liposome/neutrophils were intravenously injected (10⁷ neutrophils per mouse) to LPS
751 treated mice. Free MTX, MTX-liposomes (an equivalent amount of 2µg of MTX per mouse)
752 and blank neutrophils (10⁷ per mouse) were also injected *i.v.* to LPS injected mice as control
753 groups and model mice without any treatment as the untreated control group. An extra 24 h
754 after neutrophil *i.v.* injection, mice from five groups were sacrificed and the quadriceps from
755 left healthy legs and right LPS injected legs were taken out. All the quadriceps were weighed
756 and lysed in Cell Lysis Buffer 2 (R&D Systems) for 30 min at 37 °C. The supernatant was
757 collected after centrifugation. Three different inflammatory cytokines IL-1 α, TNF- α and IL-6
758 in the supernatant were quantified using Magnetic Luminex Assay (R&D Systems).

759 *Myocardial IRI model and fluorescence molecular tomography*

760 Female CD-1 mice (4-5 weeks old) were anaesthetised with 4% isoflurane and then maintained
761 at 2% in 100% O₂. Mice received 0.024 mg buprenorphine subcutaneously (1.1 mg kg⁻¹;
762 Vetergesic, Alstoe Animal Health, UK), and were placed on a supine position, and intubated

763 and ventilated with a tidal volume of 250 μL and a respiratory rate of 150 breaths min^{-1} (Hugo-
764 Sachs MiniVent type 845; Harvard Apparatus Ltd., Kent, UK). The chest was shaved and a skin
765 disinfectant was applied. A film dressing was placed over the chest to prevent furs entering the
766 wound. After a left thoracotomy in the fourth intercostal space, the pericardium was removed,
767 a 6-0 polyethylene suture was used to ensnare the left anterior descending (LAD) and tied
768 against a polythene tubing for 60 min (LAD ischaemia) after which the ligating suture was
769 loosened to allow reperfusion. The ligature was consistently positioned $\sim 1\text{mm}$ below the atrio-
770 ventricular junction. At the end of surgery mice were given 0.5 mL saline by subcutaneous
771 injection to counter dehydration and allowed to recover in a heated chamber for 20 min, then
772 moved to a normal holding cage with supplemental heat for a few hours and mashed food at
773 floor level. Adequate post-operative care was provided. Electrocardiogram (ECG), heart rate
774 and body temperature were monitored throughout surgery. Consistency of the surgical IRI
775 model was ensured by application of pre-defined surgical exclusion criteria: clear ST segment
776 elevation on the ECG and distinct blanching of the myocardium after LAD ligation are primary
777 criteria used to confirm the occurrence of myocardial infarction.

778 To determine the biodistribution of injected neutrophils in mice with myocardial IRI, 24 h after
779 reperfusion, neutrophils were isolated from donor mice, labelled with VivoTrack 680 and
780 intravenously injected to mice with myocardial IRI (3.36×10^6 neutrophils per mouse) and
781 healthy mice. 1 h and 2 h post *i.v.* injection, mice were killed and the hearts were perfused with
782 PBS and excised. Kidney, spleen, lung and liver were harvested as well for *ex vivo* imaging.
783 Five same organs from non-injected healthy mice were also harvested as the blank control. All
784 the organs were imaged using Fluorescence Molecular Tomography (FMT4000, PerkinElmer).

785 To investigate the biodistribution of liposome loaded neutrophils in mice with myocardial IRI,
786 24 h after reperfusion, formulated liposome/neutrophils (liposomes were labelled with DiD)
787 were intravenously injected to mice with myocardial IRI (5.6×10^6 neutrophils per mouse) and

788 healthy mice. 1 h post *i.v.* injection mice were killed and the hearts were perfused with PBS and
789 excised. Kidney, spleen, lung and liver were harvested and only a part of each organ was used
790 for *ex vivo* imaging. Five same organs from non-injected healthy mice were also harvested as
791 the control. All the organs were imaged using Fluorescence Molecular Tomography (FMT4000,
792 PerkinElmer). The collected fluorescence images were reconstructed by FMT 4000 system
793 software (TrueQuant v3.0, PerkinElmer) for the quantification of three-dimensional
794 fluorescence signals in different organs.

795 *Statistics*

796 All the statistical analyses were conducted in GraphPad 8.0 (Prism). All the statistical tests were
797 specified in the figure legends. Shapiro-Wilk test was used to assess normality and thus
798 determine the statistical test. For non-normal distributions, the left healthy leg and right
799 inflamed leg from the same mouse were preselected as a pair to analyse.

800

801 **Supplementary References**

- 802 [1] H. Zhang, in *Liposomes*, Springer, **2017**, pp. 17–22.
- 803 [2] U. Baxa, in *Charact. Nanoparticles Intend. Drug Deliv.*, Springer, **2018**, pp. 73–88.
- 804 [3] P. Kapusta, P. Gmbh, **2010**, 0.
- 805 [4] P. Müller, P. Schwille, T. Weidemann, *Bioinformatics* **2014**, 30, 2532.

806

807

808

809

810

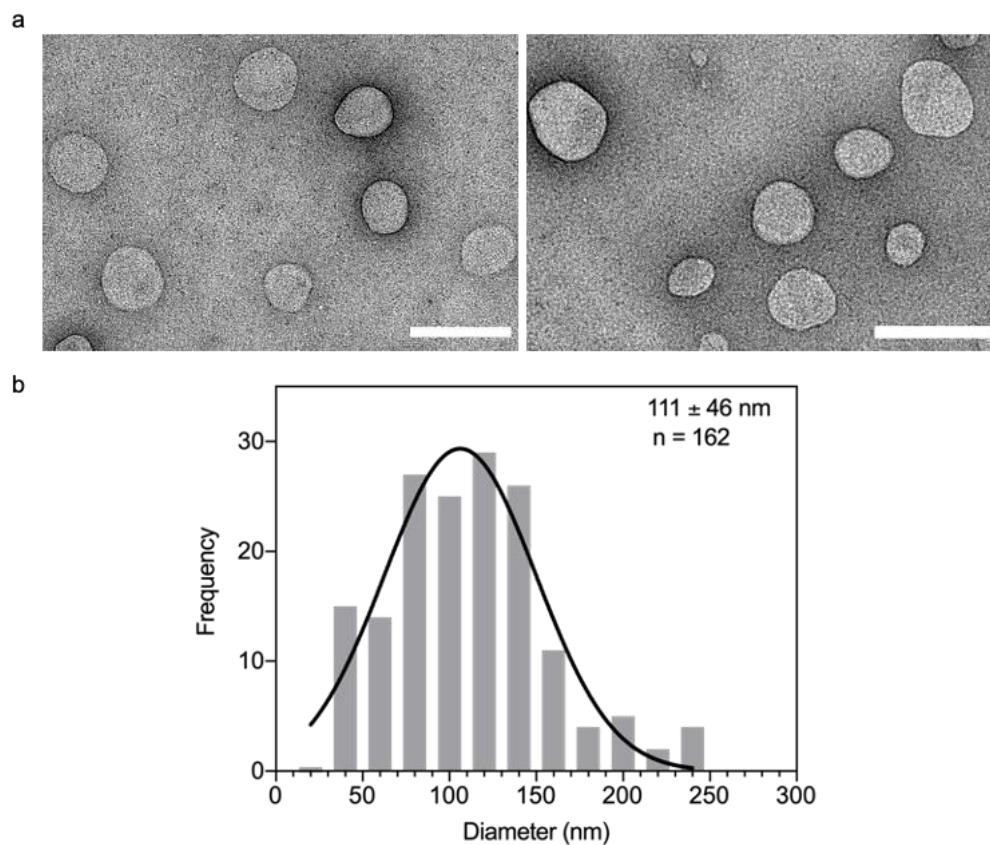
811

812

813

814

815



816

817 **Figure S1. TEM images and corresponding histogram for MTX-liposomes. a,** TEM images
818 of MTX-liposomes. Scale bar: 200 nm. **b,** Size distribution of MTX-liposomes.

819

820

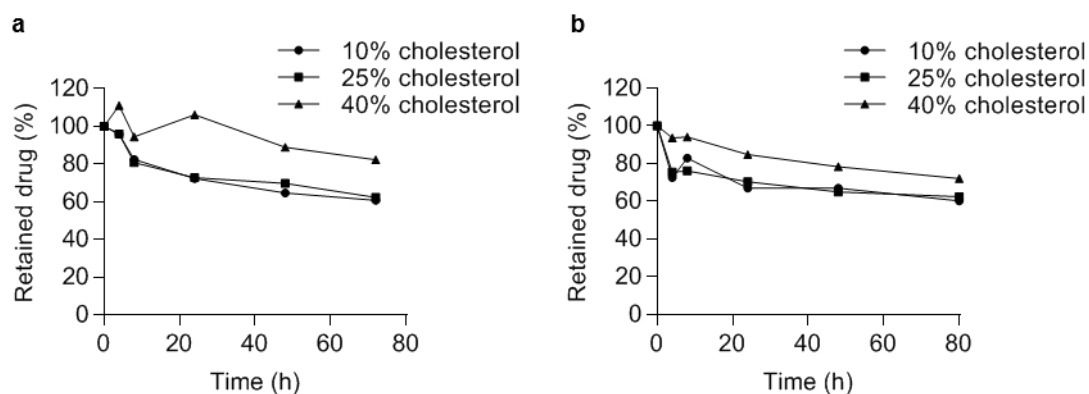
821

822

823

824

825



826

827 **Figure S2. The effect of cholesterol percentage of liposomes (liposome composition: 16:0-**

828 **18:1 PC (POPC), 18:0 TAP and cholesterol) on drug retention behaviour. Quantity of**

829 **retained drug (MTX concentration used during liposome formation: a: 5 mg mL⁻¹; b: 10 mg**

830 **mL⁻¹) inside liposomes with different cholesterol percentages over 3 days in PBS pH 7.4 at**

831 **room temperature measured by LC-MS (n = 1).**

832

833

834

835

836

837

838

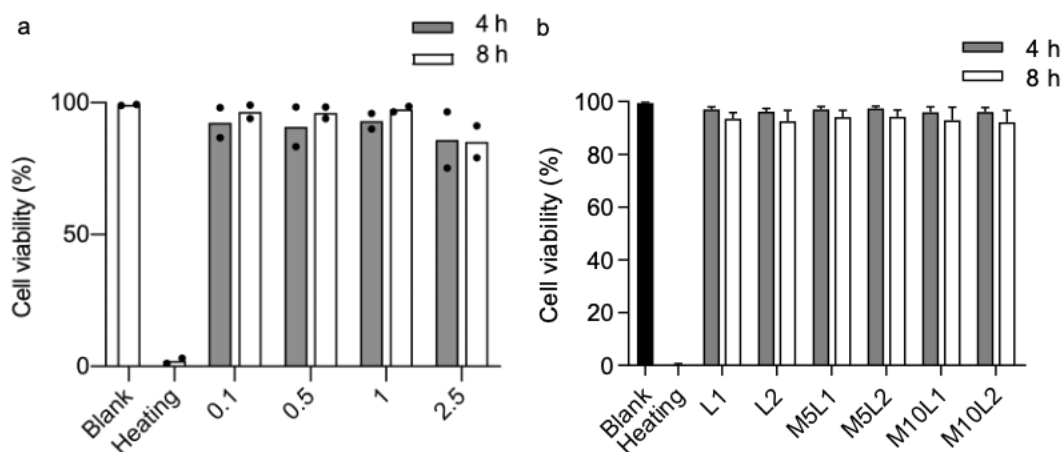
839

840

841

842

843



844

845 **Figure S3. Cytocompatibility of different liposome treatments to neutrophils after**

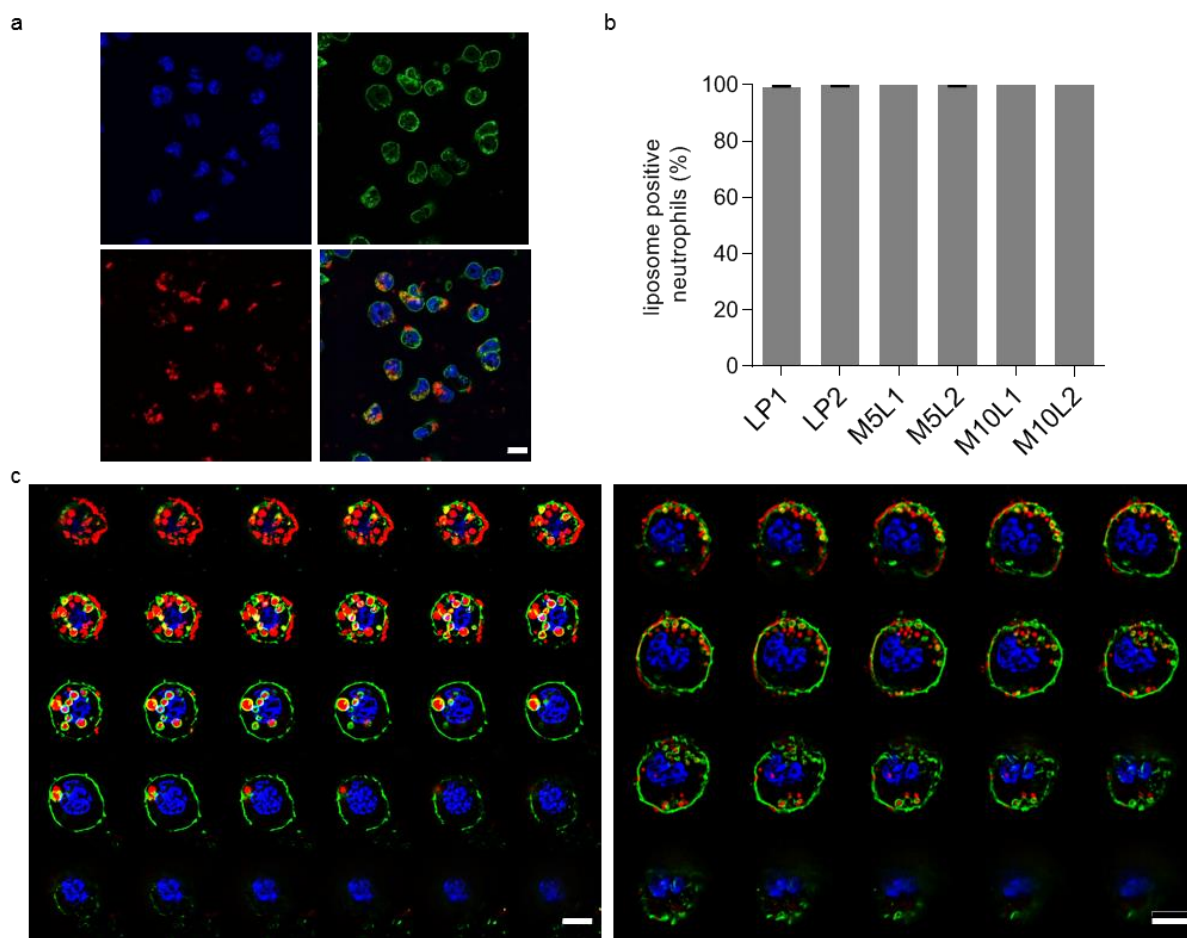
846 **incubation for 4 h and 8 h. a,** Isolated neutrophils were incubated with blank liposomes at

847 different lipid concentrations (Data shown as mean, $n = 2$). **b,** Isolated neutrophils were

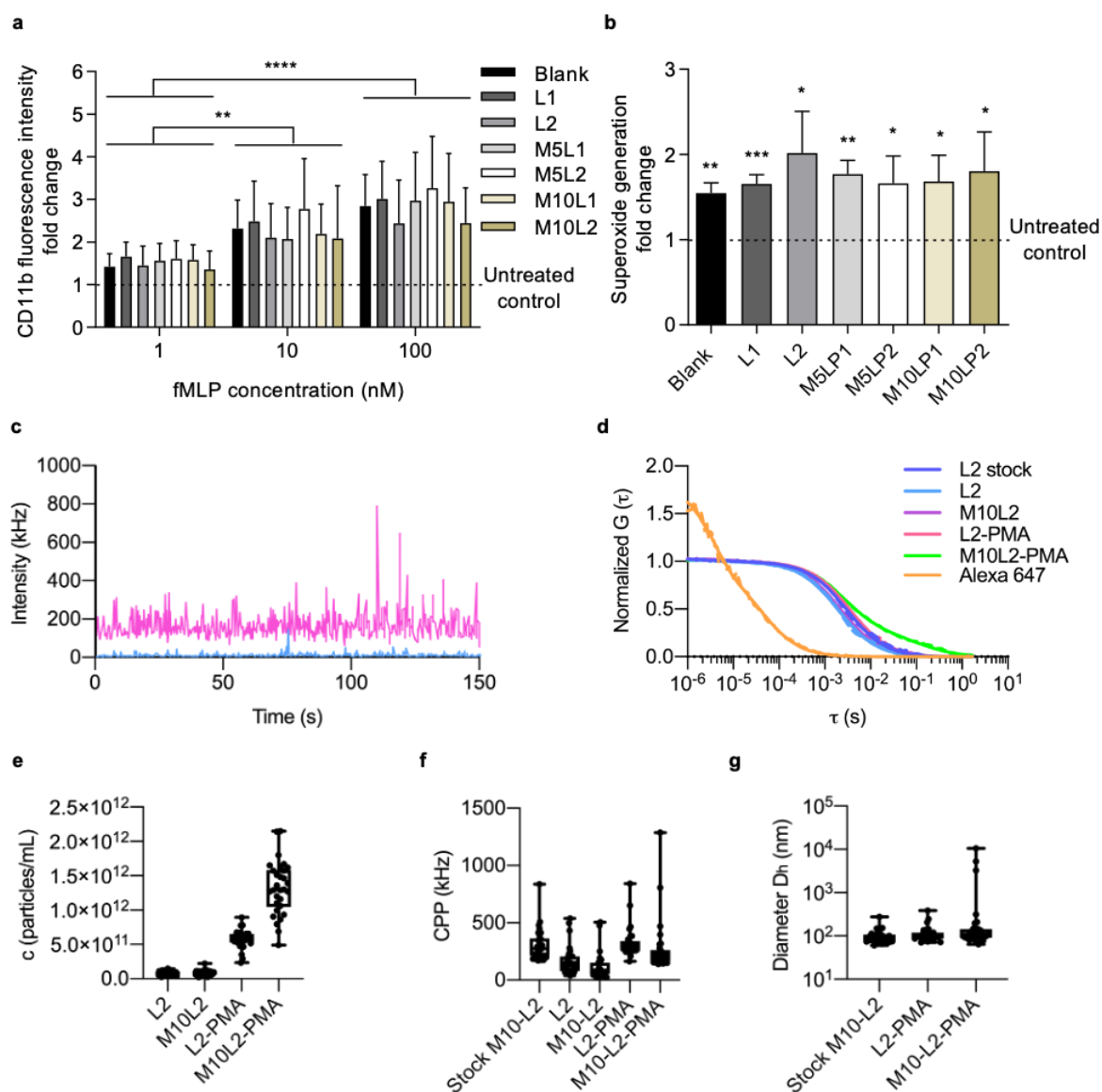
848 incubated with blank liposomes and MTX-liposomes at different lipid concentrations. Zombie

849 Green was used to measure neutrophil viability by flow cytometry. Neutrophils heated at 70 °C

850 for 10 min were used as the negative control (dead cells) (mean \pm s.d., $n = 3$).

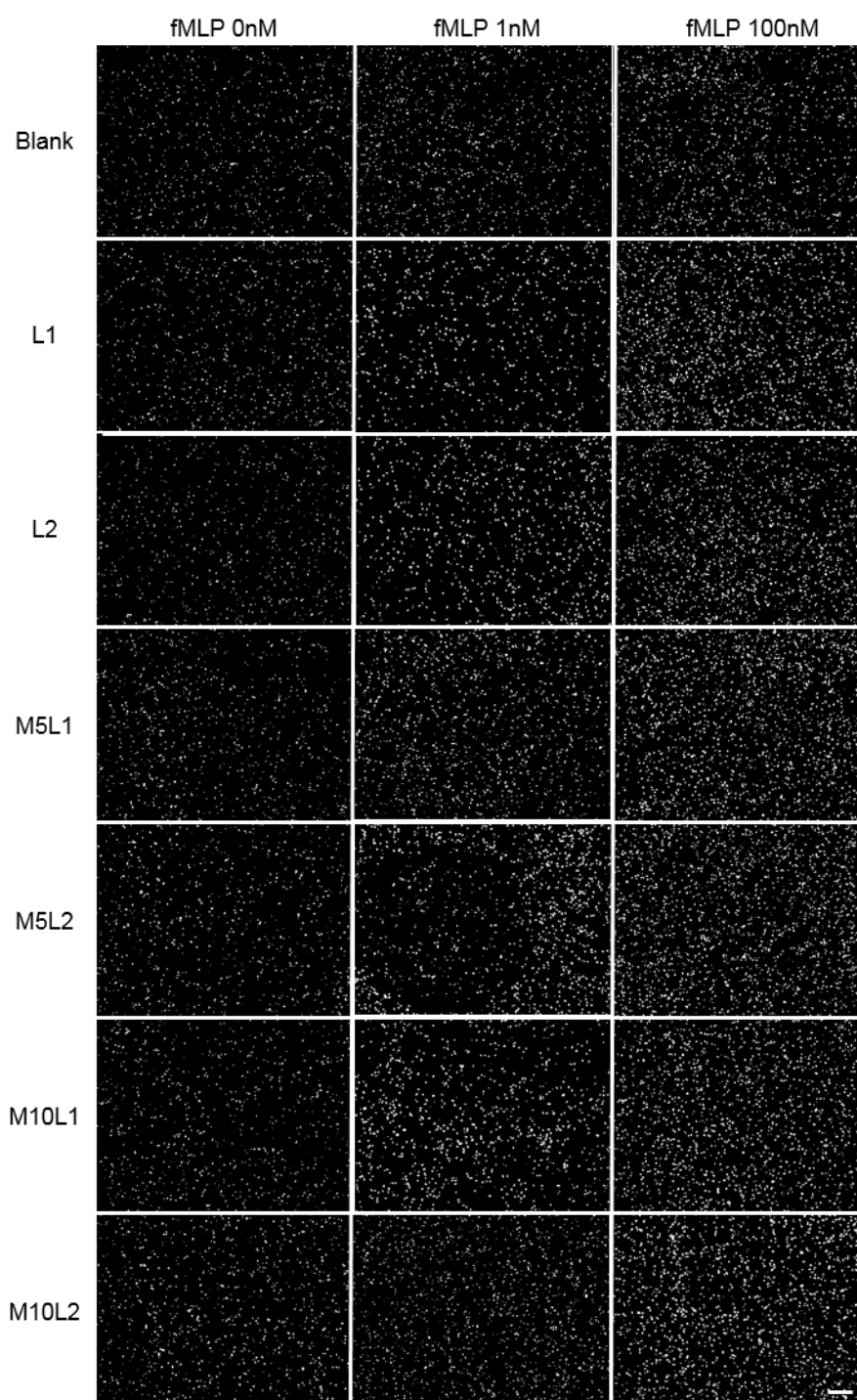


851
852 **Figure S4. Images of liposome loaded neutrophils.** a, CLSM images of MTX-liposome
853 loaded neutrophils (DiD was used to label the liposome membrane (red), WGA was used to
854 stain the cell membrane (green)). Scale bar: 10 μ m. b, Flow cytometric analysis of liposome
855 loaded neutrophils. Isolated neutrophils were incubated with blank liposomes and MTX-
856 liposomes at different lipid concentrations for 1 h (mean \pm s.d., n = 3). c, Super resolution
857 images (SIM) showing the location of MTX-liposomes (red) on/in single neutrophil at different
858 z position. Scale bars: 5 μ m.



859
 860 **Figure S5. Preservation of physiological functions of neutrophils after loading with**
 861 **different concentrations of MTX-liposomes and repeat of stimulated release of liposomes**
 862 **(DiD labelled) from neutrophils after treatment with PMA detected by FCS. a,** Change in
 863 the CD11b expression of liposome loaded neutrophils after treatment with fMLP at different
 864 concentrations. Neutrophils were loaded with blank liposomes and MTX encapsulated
 865 liposomes at different concentrations and then stained with PE anti-mouse CD11b antibody
 866 (mean \pm s.d., $n = 3$ independent experiments). $**P < 0.01$, $****P < 0.0001$, two-way ANOVA,
 867 Bonferroni post hoc test. **b,** Change in the superoxide generation of liposome loaded neutrophils
 868 with and without fMLP treatment. The superoxide level of cells was detected using

869 dihydroethidium and compared to untreated control (mean \pm s.d., $n = 3$ independent
870 experiments). * $P < 0.05$, ** $P < 0.01$, *** $P < 0.001$, unpaired two-tailed Student's t test. **c**, Raw
871 fluorescence intensity traces recorded for samples collected after incubation of
872 liposomes/neutrophils with and without stimulated release (+/- PMA). **d**, Average
873 autocorrelation curves from FCS measurements ($n = 30$ independent measurements, 5s each).
874 **e**, Amount of released liposomes given in particles per mL, **(f)** signal (counts) per particle (CPP)
875 and **(g)** hydrodynamic diameter (D_h) of liposomes was calculated from the fit parameters
876 obtained in **c**. Centre line, the median; box limits, upper and lower quartiles; whiskers,
877 minimum and maximum values ($n = 30$ measurements per sample).



878

879 **Figure S6. Images of neutrophils at the bottom side of the transwell membrane after**

880 **migration test.** Neutrophils were incubated with blank liposomes or MTX-liposomes at

881 different lipid concentrations. Formulated MTX-liposome/neutrophils were put in the upper

882 chamber of the transwell and activated by fMLP in the lower chamber. MTX-

883 liposome/neutrophils migrated through the pores of the membrane. Membranes were taken out

884 and the cells on the upper side were removed. The nuclei of neutrophils at the bottom side of

885 the membrane were stained with DAPI and imaged by fluorescence microscopy (DAPI channel).

886 Nuclei counts for the different conditions are shown in Fig 3b Scale bar: 100 μm .

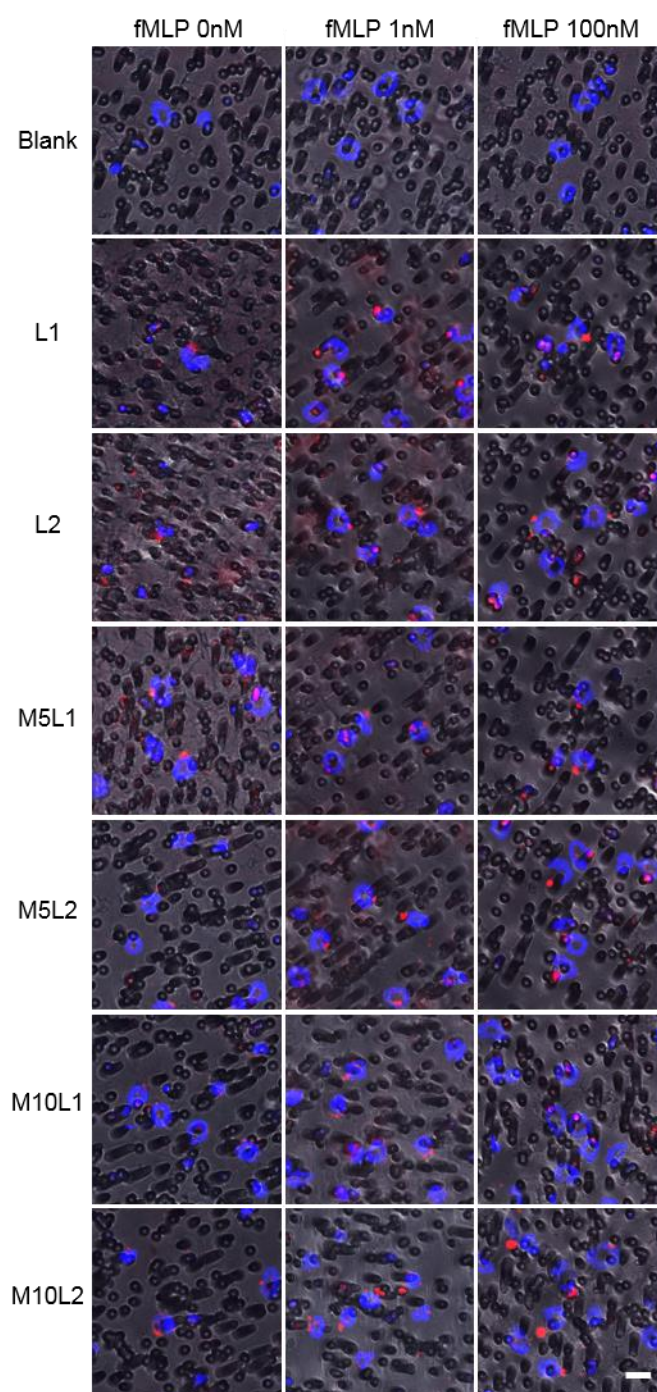
887

888

889

890

891



892

893

894 **Figure S7. CLSM images of MTX-liposome/neutrophils on the transwell membrane.**

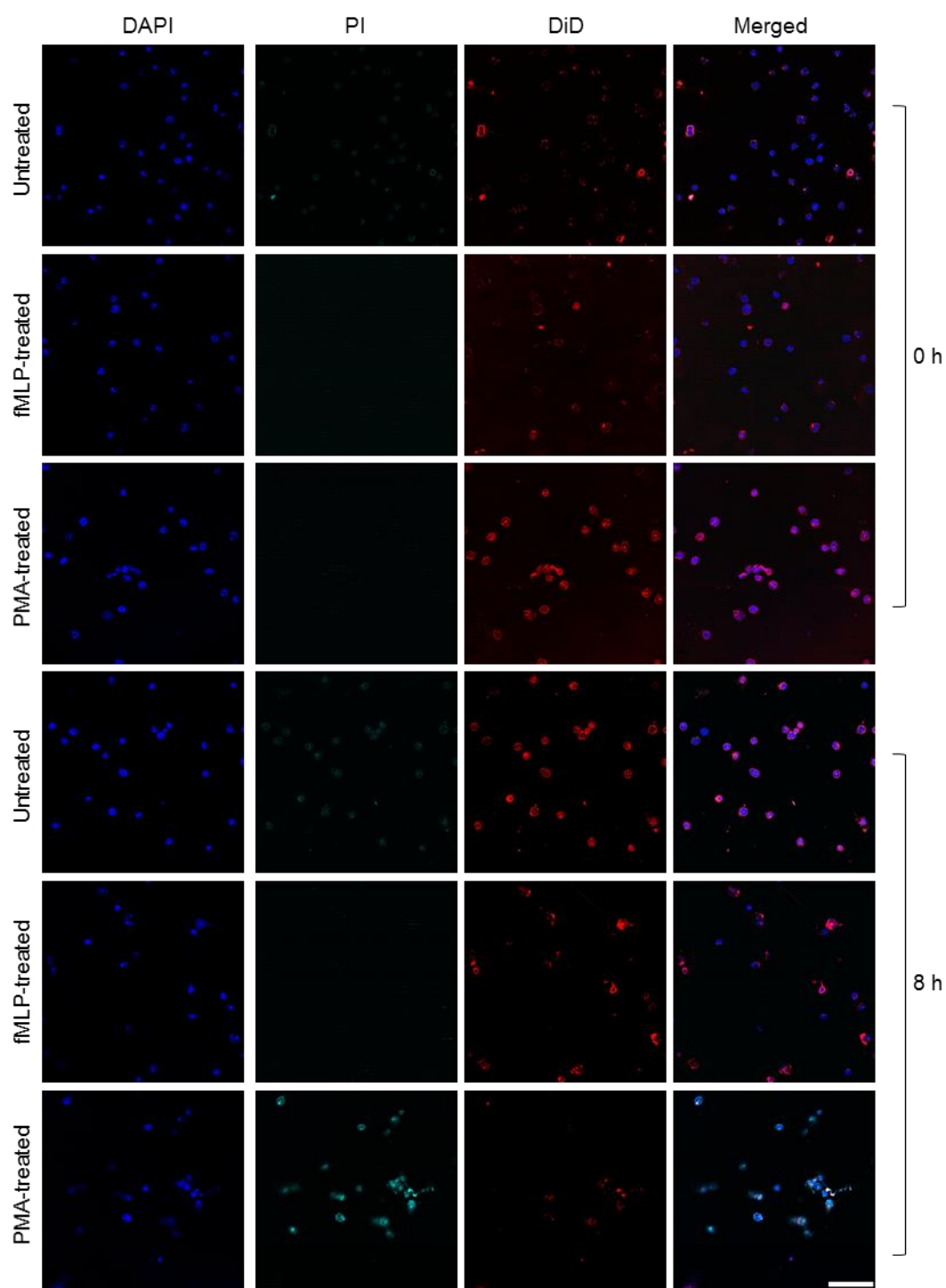
895 Formulated MTX-liposome/neutrophils (liposomes were labelled with DiD) were put in the

896 upper chamber of the transwell to measure the cell migration ability (details were described in

897 Figure S6). The membranes were cut out and put in an ibidi chamber slide and imaged using

898 confocal microscopy. Pores of the membrane (dark grey) were traversed by the liposome-

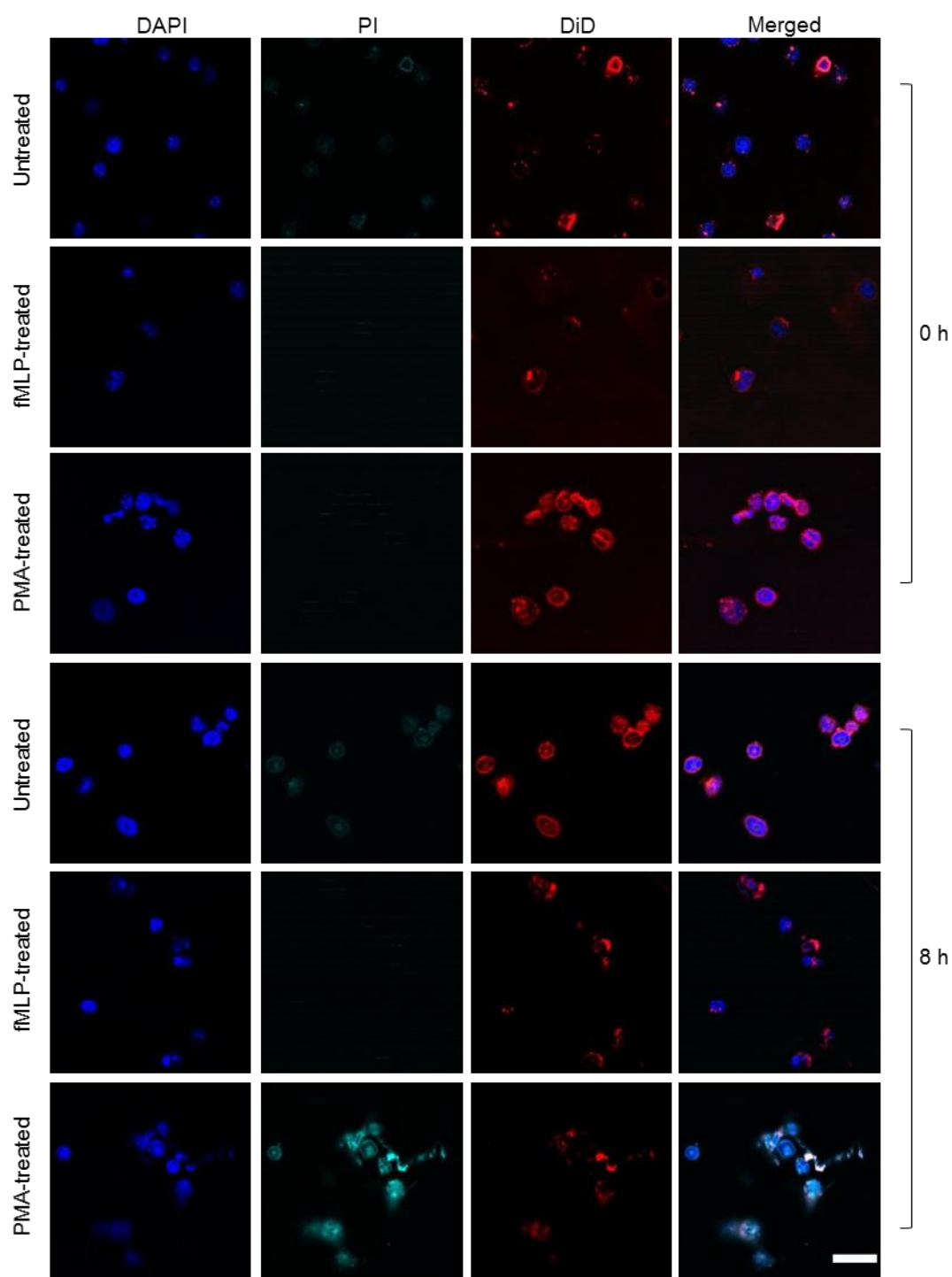
899 loaded neutrophils. Scale bars: 5 μ m.



900

901 **Figure S8. CLSM images of DiD-liposome/neutrophils before and after treatment with**
902 **fMLP or PMA.** Liposomes were labelled with DiD, followed by incubation with neutrophils
903 to form liposome/neutrophils. Formulated liposome/neutrophils were incubated in presence of
904 fMLP or PMA for 0 h and 8 h. The nuclei of neutrophils were stained with DAPI, the released

905 DNA fragments were stained with PI. The merged image is the overlay of the three individual
906 images. Scale bar: 50 μm .



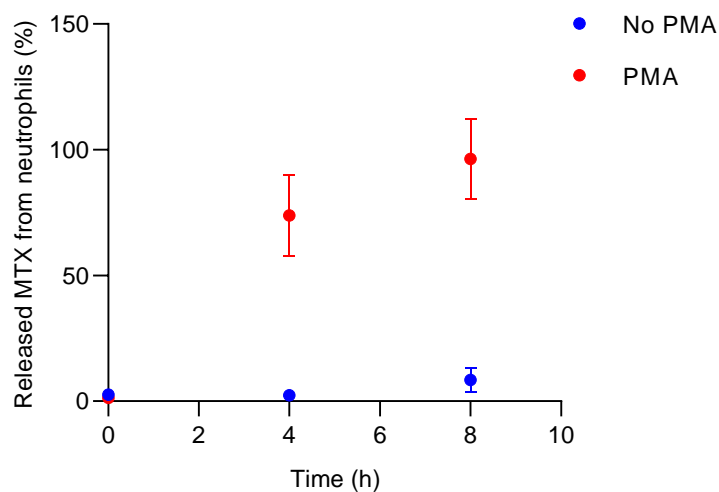
907

908 **Figure S9. Zoom of CLSM images from Figure S8. Scale bar: 10 μm .**

909

910

911



912

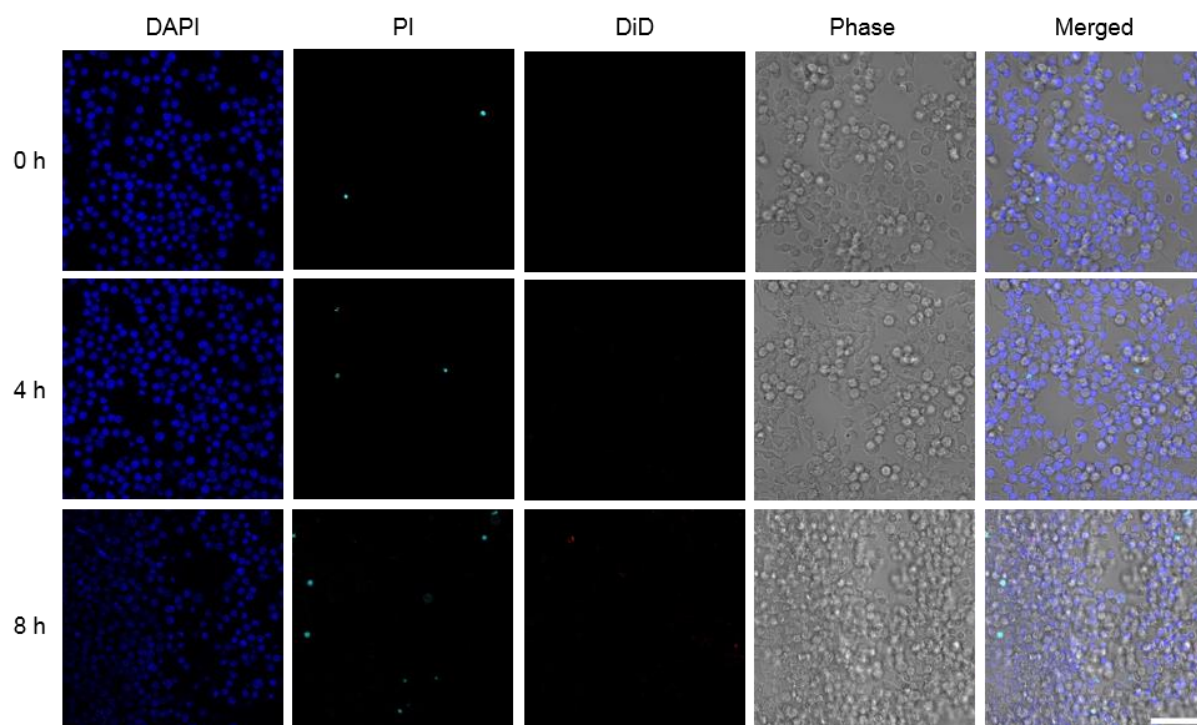
913 **Figure S10. Percentage of released MTX from neutrophils.** Formulated MTX-
914 liposome/neutrophils were incubated with and without the inflammatory stimuli (+/- PMA).
915 The supernatants were collected at different time points and released MTX in the supernatants
916 was quantified by ELISA. Data shown as mean \pm s.d., n = 3.

917

918

919

920

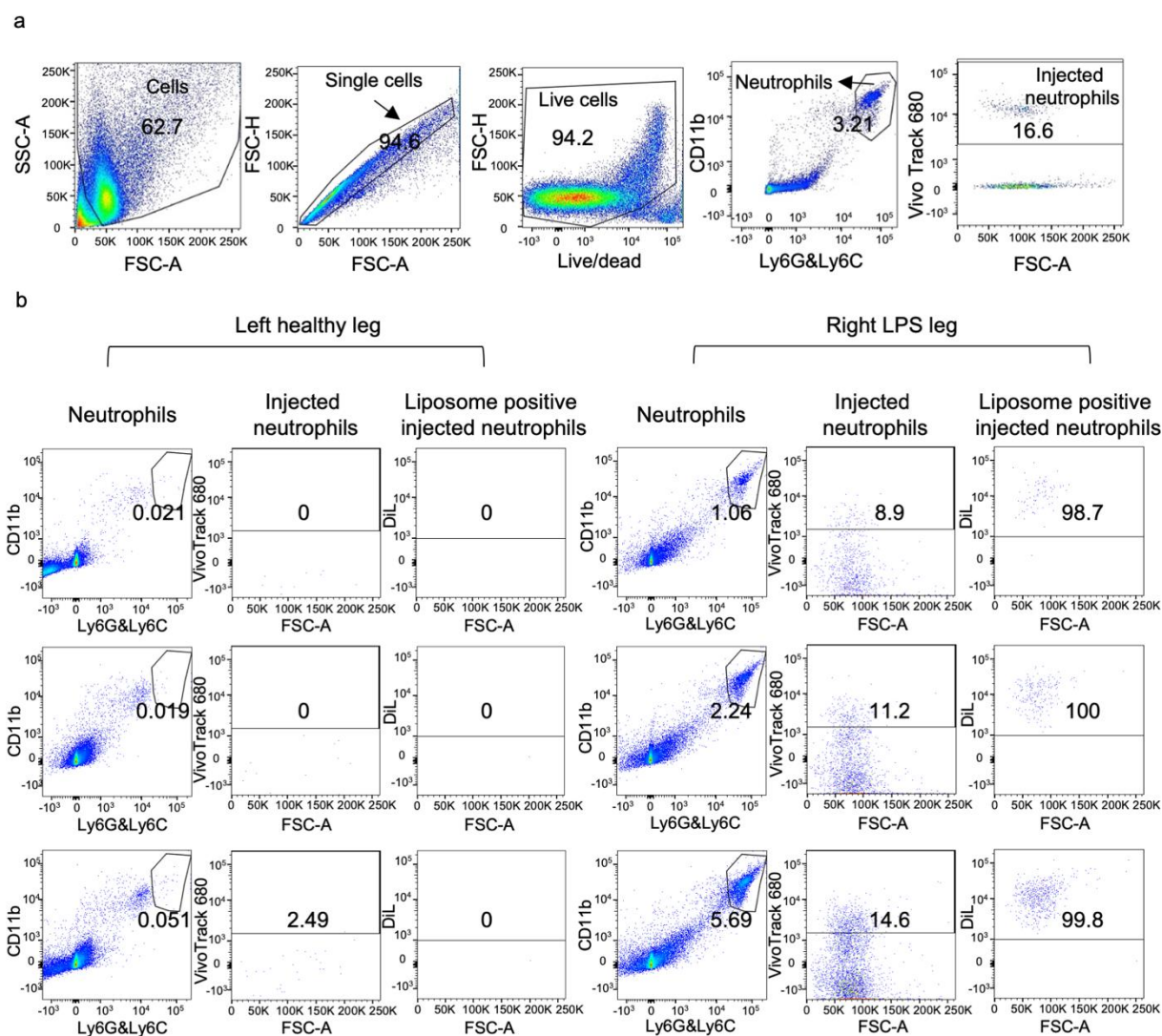


921
922 **Figure S11. CLSM images of RAW 264.7 cells after incubation with liposome/neutrophils**
923 **for 0 h, 4 h and 8 h in the absence of PMA.** The nuclei of RAW 264.7 cells were stained with
924 DAPI, the released DNA fragments were stained with PI and the liposomes were labelled with
925 DiD. The merged image is the overlay of the four individual images. Scale bar: 50 μm .

926

927

928



929

930 **Figure S12. The targeting effect of liposome/neutrophils to the inflamed quadriceps. a, An**931 example showing the gating strategy (data have been shown in Figure 4b). **b, Flow cytometric**

932 analysis of the healthy quadriceps and the inflamed quadriceps after injection of liposome

933 loaded neutrophils (liposomes were labelled with DiL; neutrophils were labelled with

934 VivoTrack 680). First column: gate shows the double positive population of neutrophils within

935 overall cell population. Second column: gate shows the VivoTrack 680 positive population of

936 injection neutrophils compared to the total neutrophil population. Third column: gate shows

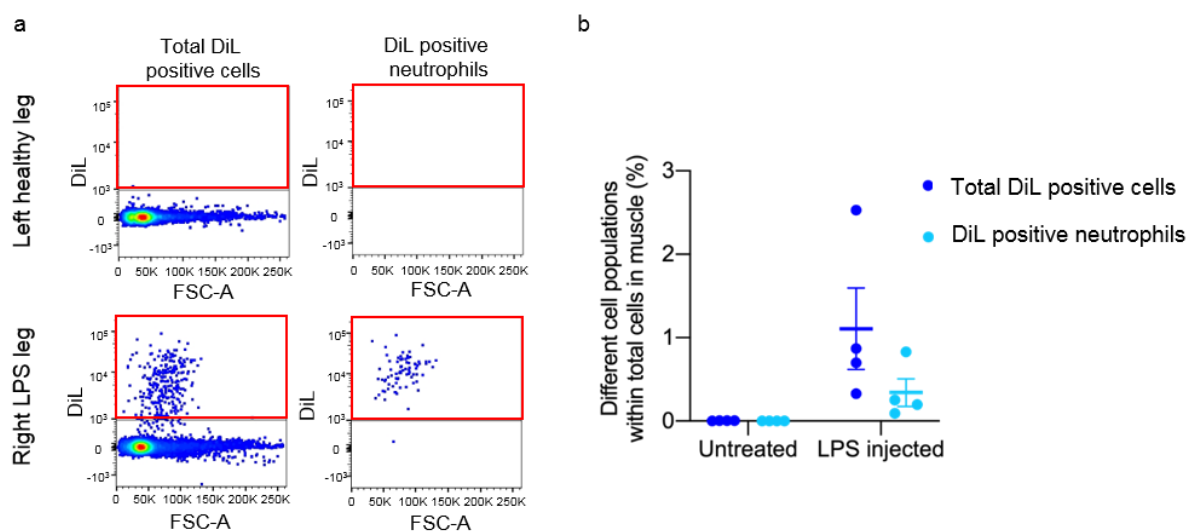
937 DiL positive population of liposome in neutrophils compared to the total injected neutrophil

938 population.

939

940

941



942

943 **Figure S13. Delivery of cargo (DiL) to non-neutrophil cells via the liposome**944 **(DiL)/neutrophil system. a, Flow cytometric analysis of DiL positive cell populations in the**945 **healthy quadriceps and the inflamed quadriceps after injection of liposome loaded neutrophils**946 **(liposomes were loaded with DiL). Gates (red) showing populations of total DiL positive cells**947 **(include DiL positive neutrophils) and DiL positive injected neutrophils (CD11b+Ly6G/6C+)**948 **in the healthy quadriceps and LPS-injected quadriceps. b, The percentage of total DiL positive**949 **cells and DiL positive injected neutrophils among total cells digested from the quadriceps.**

950

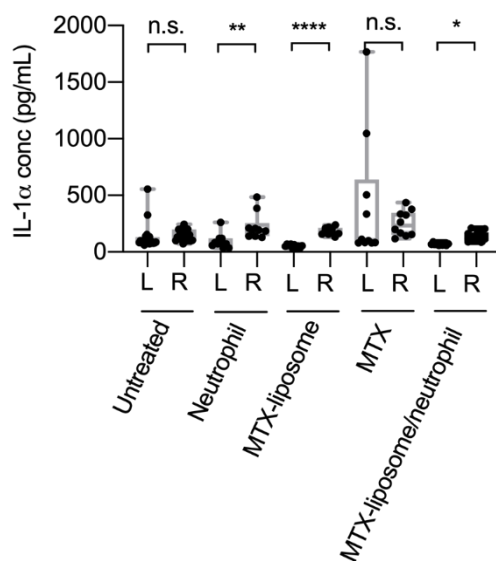
951

952

953

954

958



959

960 **Figure S14. IL-1 α level in the healthy quadriceps and LPS-injected quadriceps after**
961 **different treatments.** Centre line, the median; box limits, upper and lower quartiles; whiskers,
962 minimum and maximum values. **P < 0.01, ****P < 0.0001, n.s. not significant, Kruskal-
963 Wallis, Corrected Dunn's post hoc test, n = 20 in the untreated group, n = 10 in other treated
964 groups.

965

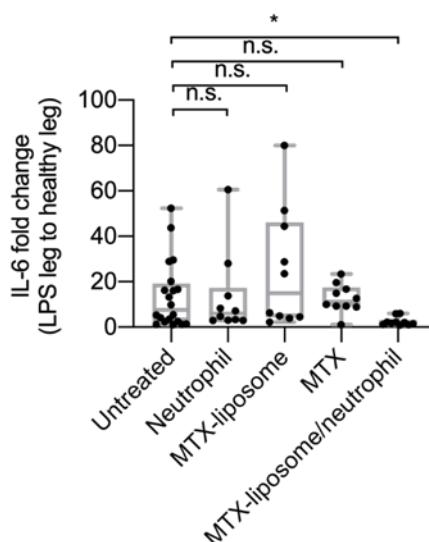
966

967

968

969

970



971

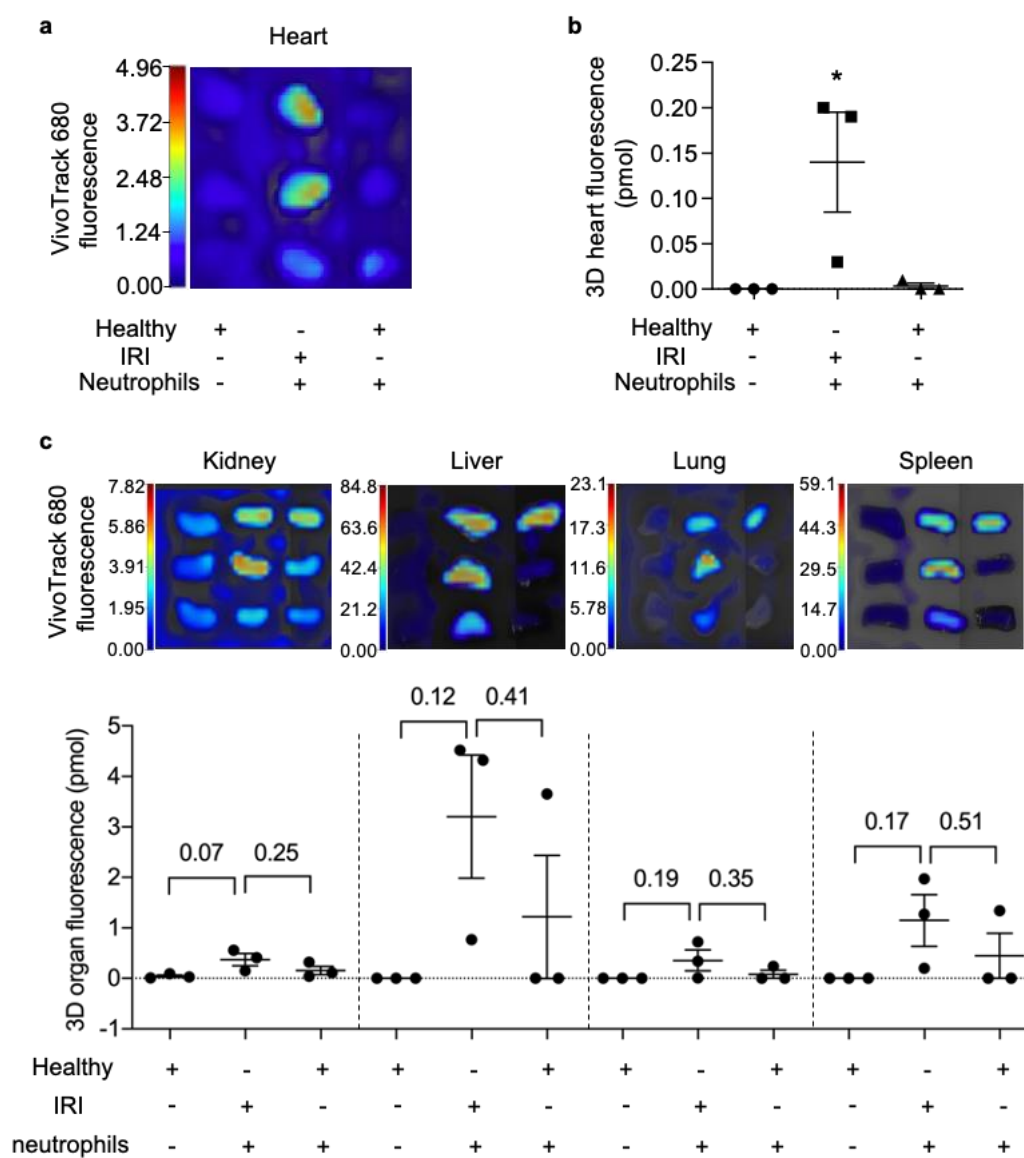
972 **Figure S15. IL-6 levels in inflamed versus healthy quadriceps after different treatments.**

973 Fold-change of IL-6 expression level in LPS injected versus non-injected quadriceps. Centre

974 line, the median; box limits, upper and lower quartiles; whiskers, minimum and maximum

975 values, n = 20 in the untreated group, n = 10 in other treated groups. * $P < 0.05$, ** $P < 0.01$,

976 Kruskal-Wallis, Corrected Dunn's post hoc test.



977

978 **Figure S16. *In vivo* accumulation of injected neutrophils (labelled with VivoTrack 680) in**

979 **the heart after myocardial IRI surgery and biodistribution in other organs at 1 h post**

980 **neutrophil injection. a, Fluorescence image of hearts from mice after different treatments. b,**

981 **Total amount of VivoTrack 680 dye in hearts (pmol, mean \pm s.e.m.). *P < 0.05, one way**

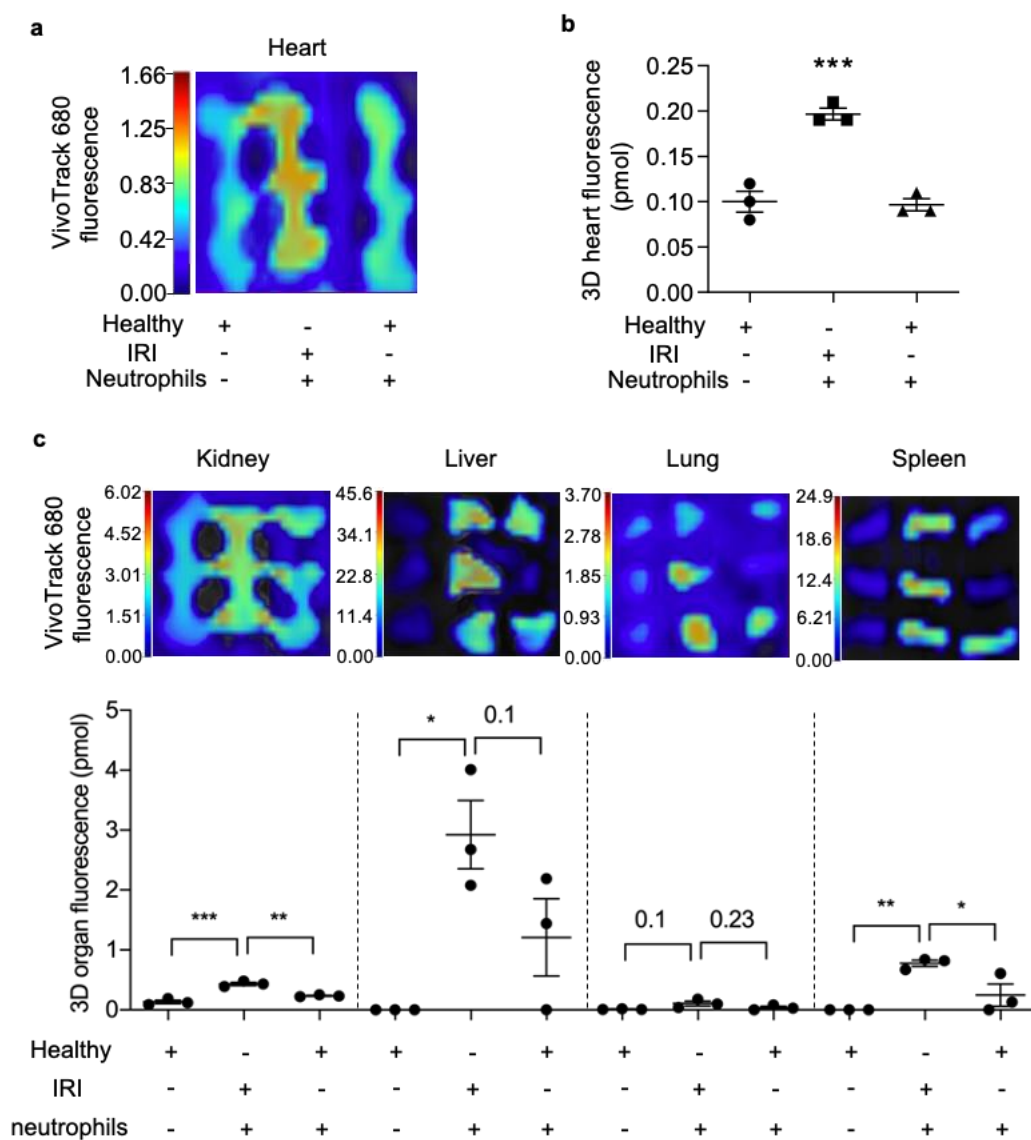
982 **ANOVA, Bonferroni post hoc test, n = 3. c, *In vivo* biodistribution of injected neutrophils in**

983 **kidney, liver, lung and spleen (from left to right). Top row: fluorescence images of different**

984 **organs from corresponding mice. Bottom row: total amount of VivoTrack 680 dye in different**

985 **organs (pmol, mean \pm s.e.m.). One-way ANOVA, Bonferroni post hoc test, n = 3.**

986



987

988 **Figure S17. *In vivo* accumulation of injected neutrophils (labelled with VivoTrack 680) in**

989 **the heart after myocardial IRI surgery and biodistribution in other organs at 2 h post**

990 **neutrophil injection. a,** Fluorescence image of hearts from mice after different treatments. **b,**

991 Total amount of VivoTrack 680 dye in hearts (pmol, mean \pm s.e.m.). *** $P < 0.001$, one way

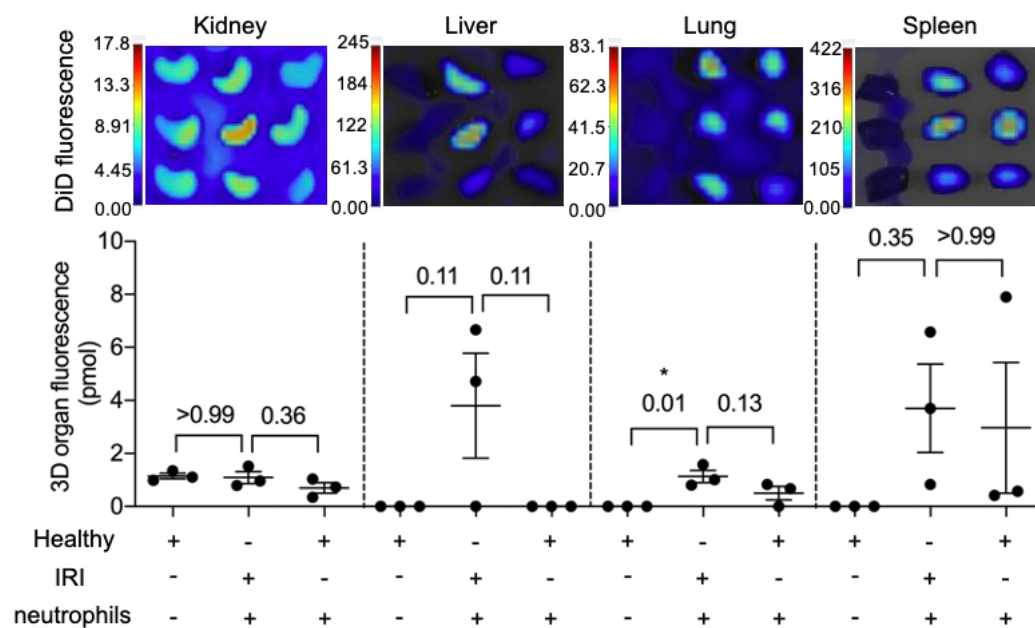
992 ANOVA, Bonferroni post hoc test, $n = 3$. **c,** *In vivo* biodistribution of injected neutrophils in

993 kidney, liver, lung and spleen (from left to right). Top row: fluorescence images of different

994 organs from corresponding mice. Bottom row: total amount of VivoTrack 680 dye in different

995 organs (pmol, mean \pm s.e.m.). * $P < 0.05$, ** $P < 0.01$, *** $P < 0.001$, one-way ANOVA,

996 Bonferroni post hoc test, $n = 3$.



997

998 **Figure S18. *In vivo* biodistribution of liposomes in other organs in mice with myocardial**

999 **IRI at 1 h post liposome/neutrophil injection. *In vivo* biodistribution of DiD labelled**

1000 liposomes in the kidney, liver, lung and spleen (from left to right). Top row: fluorescence

1001 images of different organs from mice. Bottom row: total amount of DiD dye in the different

1002 organs (pmol, mean \pm s.e.m.). *P < 0.05, one-way ANOVA, Bonferroni post hoc test, n = 3.

1003

1004

1005

1006

1007

1008

1009